Mat. Res. Soc. Symp. Proc. **406**, 189-194 (1996).

# IMAGING OF SILICON CARRIER DYNAMICS WITH NEAR-FIELD SCANNING OPTICAL MICROSCOPY

A.H. LA ROSA, B.I. YAKOBSON, and H.D. HALLEN
Department of Physics, North Carolina State University, Raleigh, NC 27695.

## ABSTRACT

A contactless high spatial resolution technique has been developed to characterize semiconductor materials using the Near-Field Scanning Optical Microscope. The technique can be used to non-invasively measure: surface topography, defect content, and carrier lifetime variations in silicon. The success of the technique relies on the sensitive detection of changes in infrared transmission induced by local generation of free carriers using pulsed visible radiation. Here we extend the application of this technique to characterize silicon on insulator materials. We also include computer simulation results to address the role played by diffusion in the ultimate lateral resolution that can be achieved using this technique.

## INTRODUCTION

Current trends toward miniaturization of semiconductor mechanical and electronic devices have led to a demand for high spatial resolution non-invasive characterization. While a number of optical techniques satisfy the latter condition, the spatial resolution provided by conventional optical characterization tools is often too coarse to be of analytical use in meso-scale materials applications. We have developed a technique for semiconductor characterization that allows resolution beyond the far-field diffraction limit of conventional optics through exploitation of the near-field scanning optical microscope (NSOM) [1, 2]. The technique employs a time-resolved optical characterization scheme that leads to an image of defect populations and, significantly, carrier recombination rate mapping with sub-wavelength lateral resolution in silicon [3, 4]. Here we report our results in the application of this technique to characterize silicon on insulator SOI materials.

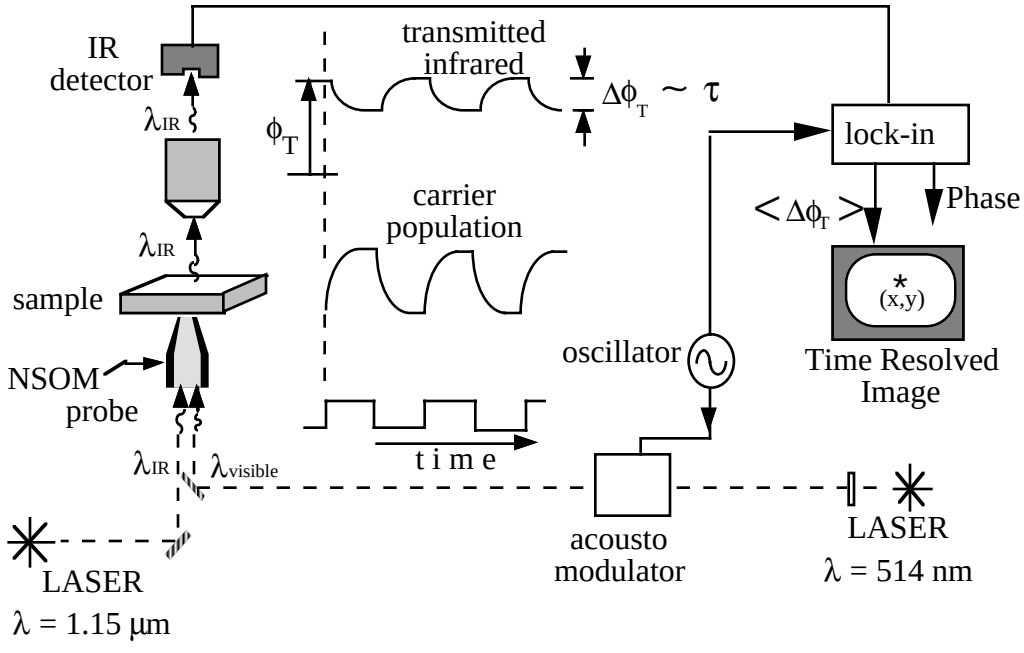


Fig. 1. Schematic (not to scale) diagram of the process to extract information of the local effective lifetime $\tau$ of excess carriers in a semiconductor. Left side: optical path of the IR radiation ($\lambda_{IR}$). Center: A timing diagram of the process. Right: Synchronous detection of the transmitted infrared signal ($\phi_T$). An image is constructed by repeating this process as the probe is scanned across the sample.

Another aspect that we address in this paper is the resolution of our measurements. In general, this technology utilizing the NSOM, appear

s. Soc. Symp. Proc. **406**, 189-194 (1996).

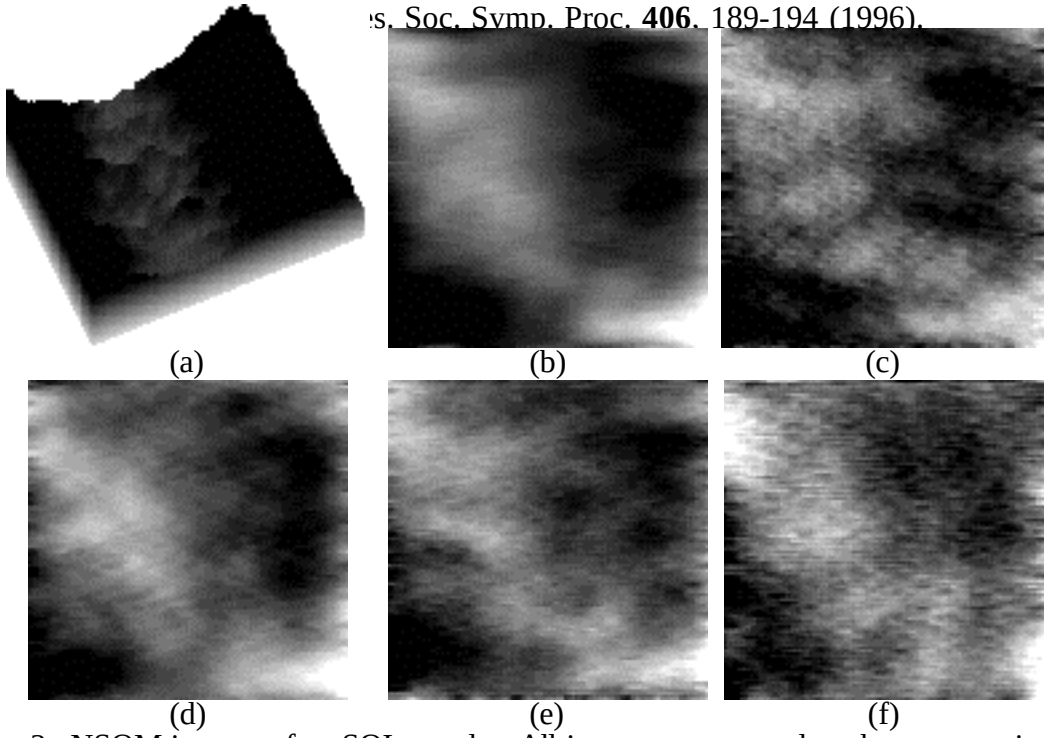


Fig. 2. NSOM images of an SOI sample. All images correspond to the same region of 7.5 μm x 7.5 μm. (a) Sample topography derived from a shear-force feedback (the gray scale range is 15 nm - black higher). (b) The infrared transmitted intensity as a function of position with 0.3 nW range and a 5 nW background subtracted. (c-f) The time-resolved images taken at the following frequencies, RMS range: (c) 170 Hz, 6.2 pW, (d) 750 Hz, 4.5 pW, (e) 8.5 kHz, 2.5 pW, and (f) 90 kHz, 0.2 pW. A strong influence of the transmitted infrared signal is observed in the time resolved images, although the resolution varies. Topographic image reveals that the thickness of either top Si or buried oxide or both vary across the analyzed region.

to have no fundamental lower size limit imposed by the sample, just that of the probe. Current limits on recombination rate variation are determined by signal/noise ratios. However, physical interpretation of high lateral resolution images may turn out a difficult task. Experimental results have already shown finer local information than would be possible if a far-field optical technique were used. We have used computer simulation studies to improve image interpretation. Our initial results are reported.

## EXPERIMENT

A previous report contains a description of the operation of the technique [5]. The experimental set up is shown schematically in figure 1. The lower and left side show the NSOM and laser sources. Visible laser light ($\lambda$ = 514 nm) is modulated by an acousto optic modulator and input to the probe. Continuous wave (CW) IR light ($\lambda$ = 1.15 μm) is also coupled through the probe. The NSOM probe consists of a sub-wavelength aperture (~100 nm here) on the end of the tapered optical fiber [6]. To attain high resolution, the NSOM probe is positioned very close to the sample (~ 5 to 10 nm) and a feedback scheme used to stabilize this distance during scanning [7, 8]. The central part in figure 1 shows a timing diagram. When the visible light in turned on, the e-h population increases until a steady state is reached (generation process). A sudden termination of the pulse is followed by a decrease in the e-h population due to a material dependent recombination process. In the simplest case, this decay follows a exponential function where a characteristic time, the carrier lifetime $\tau$, can be identified. The measurement of the local carrier lifetime, with high lateral resolution, is our focus.

Variations of the e-h population change the transmitted IR signal $\phi_T$, since free carriers absorb IR radiation. Thus we may monitor the IR transmission signal to study the e-h population

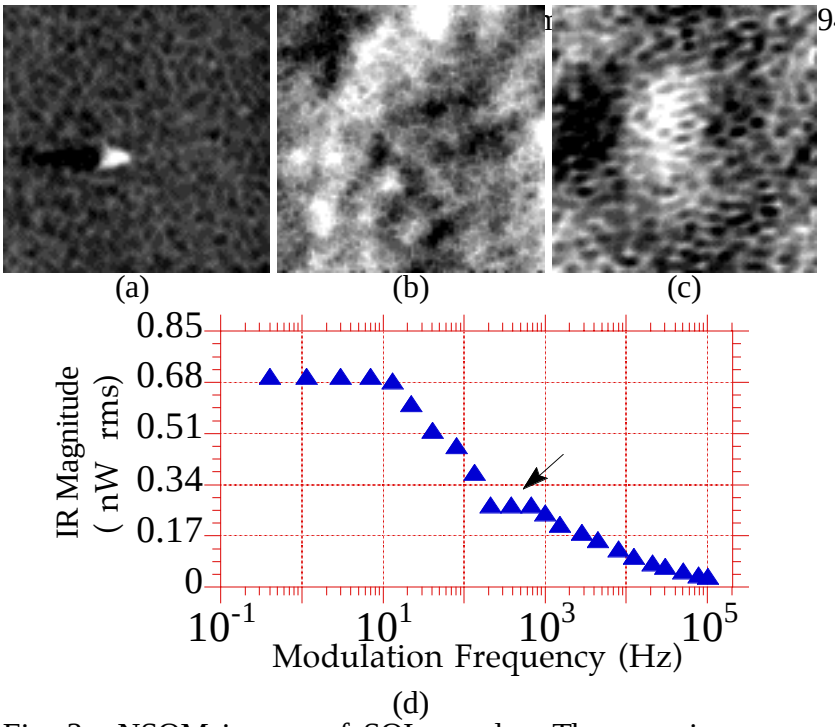


Fig. 3. NSOM images of SOI sample. The ten micron square scanned region is different from the one shown on fig. 2. (a) shows the topography range with range 50 nm, (b) shows the IR intensity with range 1.5 nW after a 21 nW background subtraction, (c) shows the time-resolved image using the phase of the modulated signal with range 24 degrees, and (d) shows the frequency dependence of the IR magnitude modulation with visible light modulation frequency. No strong correlation between the infrared transmission and the time resolved image is observed.

94 (1996).

and hence the carrier recombination process. Direct measurement of the IR signal in the time domain constitutes one way to extract values of $\tau$ provided we have acceptable signal to noise ratio. In practice, the signal levels are low, and we detect the RMS change of the IR signal shown in fig. 1 with the lock-in amplifier, since the signal magnitude $\propto \tau\cdot[1+(\omega\tau)^2]^{-1/2}$. This phase is also proportional to $\tau$ [actually *arctan* $(\omega\tau)$]. At a given position (x,y) on the sample, a signal $\langle\Delta\phi_T\rangle$ proportional to $\tau$ is generated. When the sample is subjected to a scanning process, the resulting "time resolved" image maps regions of different $\tau$. We can also generate a signal dependent upon $\tau$ by noting the phase change of the IR signal with respect to the visible pumping signal. A longer $\tau$ will effectively delay the IR signal change both while charging and during the carrier population decay.

The samples used here were silicon-on-insulator (SOI) produced by oxygen implantation and annealing. The buried oxide is ~ 400 nm thick, under ~ 120 - 130 nm of silicon. No special termination of the outer silicon surface was used. The carrier effective lifetime of this sample, $\tau$ = 1 μs, was measured at room temperature using a laser/microwave method (Lifetech-88, Semitex Co., Ltd).

## EXPERIMENTAL RESULTS

The detection scheme described above is capable of imaging the relative excess carrier lifetime or quantitatively measuring the lifetime at one point by sweeping the visible modulation frequency [4]. The images shown in figure 2 correspond to the same scanned area, a $(7.5\ \mu m)^2$ square. We present the topography and the IR transmission image for comparison, and time-resolved images taken at several visible modulation frequencies. The topography reflects surface height variations due to variations of the silicon thickness or surface layers. If several different carrier processes contributed to the recombination, one would expect the time-resolved [figure 2(c-f)] images to change to reflect the dominant process on that time scale [3]. We see that, for this sample, the time-resolved images are almost independent of the visible modulation frequency and correlate to the IR transmission image. We can understand this in the following simple model: Since the absorption coefficient of green light ($\lambda$ = 514 nm) in silicon is $\alpha \sim 10^4$ cm$^{-1}$ (light penetrates up to $\Delta z \sim 1\ \mu m$), there should be a strong influence of silicon thickness variation on the optical signals. It should be true for both the average (transmission) and time resolved signals. It seems that this geometric effect dominates the contribution from carrier modulation in this sample

region. Thus the contrast observed in the transmission image should be interpreted as thickness variations. In general, one expects a transmission image to also reflect variations in the surface conditions, however, we would not expect these to affect the time-resolved images. The contrast could also be due to defects in the silicon which absorb the IR radiation. The IR transmitted signal indicates $\Delta\phi_T / \phi_T = 6 \times 10^{-2}$. Since $\phi_T \sim \exp(-\alpha z)$, a $\Delta z$ thickness variation should induce a signal change of $\Delta\phi_T / \phi_T = \alpha \Delta z$. From here we obtain $\Delta z \sim 60$ nm, a value that is in agreement with the order of magnitude changes of the topographic image.

Fig. 3 shows NSOM images of another region of the same SOI wafer. This time no major change in the topography is observed except for a dust particle near the center. The contrast observed in the transmission signal does not correlate to the time-resolved images and may come from inhomogeneities in the other side of the silicon-substrate interphase and/or surface layers. Time resolved images utilizing the RMS magnitude change revealed little contrast due to the short lifetime in this region. We therefore used the phase of the IR signal to generate the time-resolved image shown in figure 3(c). We can estimate the local lifetime from the data in figure 3(d) and its variation from the range of figure 3(c). The knee at ~1 kHz indicated by the arrow is due to the carrier lifetime. The overall decrease is due to another, slower, process [9, 10]. We can estimate the lifetime $\tau = 1/2\pi f \sim 160$ μsec and its variation at the knee from $\Delta\tau = \Delta\phi/\omega_{knee} = 67$ μsec for the 24° phase variation measured.

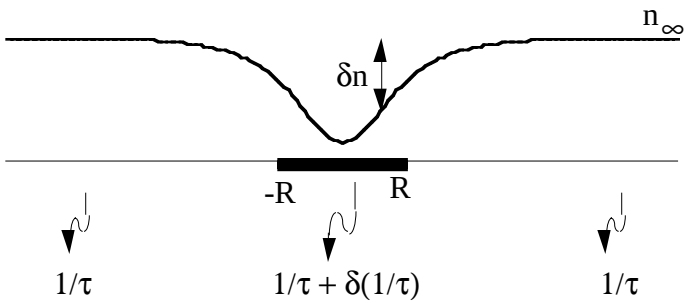


Fig. 4. The carrier concentration profile δn is shown as calculated near a region with a faster recombination rate.

## DIFFUSION OF CARRIERS

To obtain a quantitative connection between the time-resolved image contrast and the variation of the local time constant, we must use a theoretical model which accounts for the diffusion of carriers. This simple model also allows us to investigate the limits to resolution and the trade-offs between signal level and time constant resolution. The parameter which we measure is the local concentration of the excess carriers. It's further interpretation in terms of local *kinetic coefficients* - lifetime and diffusion coefficient - is affected by the mobility of carriers. Indeed, the diffusion coefficient in crystalline silicon is $D=10$ cm$^2$/s and within a (short) lifetime of just one microsecond, the diffusion length $(D\tau)^{1/2} \approx 30$ μm is much greater then the size of features to be resolved. Therefore, the mobile carriers concentration at certain point is determined by relaxation rates in an extensive surrounding domain. Nevertheless, as our data demonstrate and a simple argument below corroborates, detectable variations are observable due to changes in a local area, much smaller then $(D\tau)^{1/2}$.

Consider a domain in the sample of some size R, within which the local relaxation is somewhat faster then elsewhere around it (figure 4). Under steady illumination, the resulting steady-state concentration in the vicinity of this domain will be by δn lower then that ($n_o$) far away. An excessive decay of carriers within R should be balanced by their arrival rate, i.e,

$$\frac{4}{3}\,\pi R^3 n_o \cdot \delta(1/\tau) = 4\pi R^2 D \cdot \nabla n \qquad (1)$$

This equation results in a concentration profile at $r > R$,

Mat. Res. Soc. Symp. Proc. **406**, 189-194 (1996).

$$\delta n = A\,\frac{1}{r} \quad \text{where} \quad A = \frac{R^3\, n_o}{3\ D}\cdot\delta(1/\tau) \tag{2}$$

Therefore, the spatial scale of this variation remains of the order of R, while its magnitude depends on the variations in local lifetime $\tau$ and is inversely proportional to the mobility of carriers. With typical numerical values and for R = 100 nm, one gets variations in concentration well below 1%, as is observed. The high mobility makes the detection of small features demanding in terms of signal level, but the spatial resolution remains possible, at least for simple open geometries.

This can be illustrated by the computer simulation, which also allows us to consider more complex geometries of defect domains. The excess carrier population $n(\mathbf{x},t)$ created by the visible light pump is governed by the kinetic equation

$$\partial n(\mathbf{x},t)/\partial t = q\cdot P(\mathbf{x},t) + \iiint T(\mathbf{x},\mathbf{x'})\cdot n(\mathbf{x'},t)\cdot d^3\mathbf{x'} - n(\mathbf{x},t) / \tau(\mathbf{x}), \tag{3}$$

where the first term is the rate of generation by the pump-probe, the second describes the transport of carriers and the third one represents the local lifetime $\tau(\mathbf{x})$. $P(\mathbf{x},t)$ is the density of illumination power, and q is the quantum yield for the visible light. The absorption of the infrared component, due to local concentration $n(\mathbf{x},t)$, is then proportional to the spatial convolution in the vicinity of the probe aperture, $A(\mathbf{x_0}) = \int_a A(\mathbf{x_0},\mathbf{x})\cdot n(\mathbf{x},t)\cdot d^3\mathbf{x'}$. If the mean-free-path is shorter than the length-scale of interest (e.g. the resolution claimed) then the transport integral reduces to the usual diffusion term *div* [$D(\mathbf{x})$ *grad* $n(\mathbf{x},t)$]. Imaging $n(\mathbf{x},t)$ with NSOM probe gives information about lifetime variations due to variations in defect concentration. Generally, however, the picture is largely smeared by the motion of carriers. Assuming a certain model defect distribution, the solution of this equation allows a simulation of the carrier evolution and a calculation of the probe-collected signal for every pixel at different locations across the sample. Fig. 5 presents the IR-transparency under steady and uniform illumination by visible light. The feature to be imaged is characterized by 10-20 times shorter local lifetime, and is shaped as the letter "F". As one could expect, the higher mobility of carriers results in a less distinct image. Nevertheless, the signal profiling allows an unambiguous extraction of a diameter for the defect-filled domain. A less trivial observation is that the internal details of the imaged structure appear to be lost and can not be restored by a simple contrast enhancement: the more than three times greater contrast in fig. 4e still does not allow identification the written-in pattern.

## CONCLUSIONS

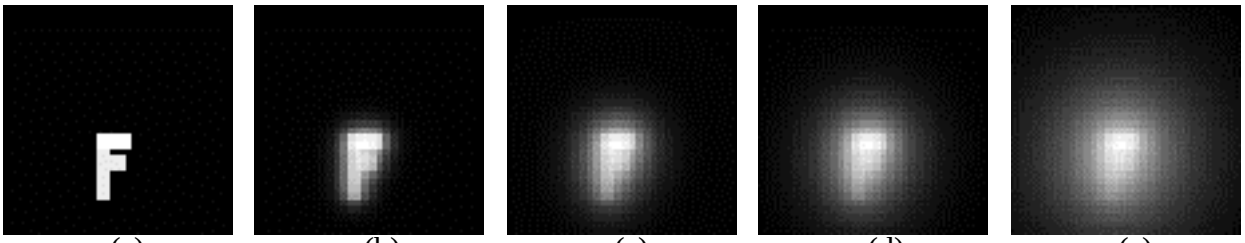


Fig. 5. A sample of simulated infrared transmittance-images under the uniform illumination by a visible light. The carriers relaxation rate is 10-20 times faster within the F-letter than elsewhere. The background lifetime of 1 μs and the frame size of 10 μm would correspond to the largest diffusion coefficient of $D_o$ = 1 $cm^2/s$ in this simulation. The effective diffusion coefficient, and scaling onto the gray range vary from D=0, gray range relative scale GRRS=1 (a), to D = $0.02D_o$, GRRS=1.05 (b), to D = $0.1D_o$, GRRS=1.3 (c) to D = $0.25D_o$, GRRS=1.7 (d), and top D = $D_o$, GRRS=3.2 (e).

We have illustrated the applicability of a novel technique for locating defects in semiconductors through their effect on the recombination of excess carriers. The all-optical method is shown to provide such data at subwavelength dimensions. A model has been developed to quantify the image contrast and understand the effects of diffusion on the signal levels and resolution of the technique. Limitations are identified in the temporal and spatial resolution. The temporal resolution is given by the detector speed. The spatial resolution is given by a combination of the NSOM probe (which can be improved), the signal level, and the effects of diffusion, which tend not to increase the overall feature size, but may obscure the internal structure of a defect with complicated topology.

## ACKNOWLEDGMENTS

We thank Michael Paesler for useful discussions. This work was supported by the U.S. Army Research Office through grants DAAH04-94-G-0156, DAAH04-94-G-0064 and DAAH04-93-G-0194.

## REFERENCES

[1] E. Betzig and J.K. Trautman, Science **257**, 189 (1992).

[2] D.W. Pohl, W. Denk and M. Lanz, Applied Physics Letters **44**, 651 (1984).

[3] A.H. LaRosa, B.I. Yakobson and H.D. Hallen, submitted (1995).

[4] A.H. LaRosa, C.L. Jahncke and H.D. Hallen, SPIE Proceedings **2384**, 101 (1995).

[5] A. LaRosa, C.L. Jahncke and H.D. Hallen, Ultramicroscopy **57**, 303 (1995).

[6] B.I. Yakobson, P.J. Moyer and M.A. Paesler, J. Appl. Phys. **73**, 7984 (1993).

[7] R. Toledo-Crow, P. C. Yang, Y. Chen and M. Vaez-Iravani, Applied Physics Letters **60**, 2957 (1992).

[8] E. Betzig, P.L. Finn and J.S. Weiner, Applied Physics Letters **60**, 2484 (1992).

[9] A. H. LaRosa, B. I. Yakobson and H. D. Hallen, Appl. Phys. Lett. **67**, (1995).

[10] H.D. Hallen, B.I. Yakobson, A. LaRosa and M.A. Paesler, SPIE **2535**, 34 (1995).